ELSEVIER

Surface Science 327 (1995) 321–329

surface science

The temperature dependent growth mode of nickel on the basal plane of graphite

M. Bäumer *, J. Libuda, H.-J. Freund

Lehrstuhl für Physikalische Chemie I, Ruhr-Universität Bochum, Universitätsstrasse 150, D-44780 Bochum, Germany

Received 26 September 1994; accepted for publication 19 December 1994

Abstract

The growth mode of metals on weakly interacting substrates is still a matter of debate. Especially for graphite this question is unsettled. In order to contribute to a clarification, we investigated the temperature dependent growth behaviour of nickel on the basal plane of graphite. Via SPA-LEED (spot profile analysis low energy electron diffraction) we found that Ni(111) islands are formed at 90 K. The formation of these islands deposited originally at 10^{-2} ML/s, however, is a rather slow process, which takes approximately two hours as observed in the profile of the (00) beam. The driving force for this rearrangement taking place after deposition is certainly the small mismatch between the lattice constant of Ni(111) and the basal plane of graphite. Furthermore, XPS has been used to determine the coverage and the height of the Ni(111) islands. At 300 K, much larger clusters with a different shape and structure are growing on the surface. It is likely that they represent the thermodynamically stable situation.

Keywords: Carbon; Growth; Low energy electron diffraction (LEED); Nickel; X-ray photoelectron spectroscopy

1. Introduction

Metal clustering on surfaces has attracted a lot of attention during the last few years (see Ref. [1], and references therein). Nevertheless, the growth behaviour of metals on weakly interacting substrates like graphite and several oxides is still a matter of debate. Whereas three-dimensional clustering is always observed in the state of thermodynamic equilibrium [2], very little is known about the growth mode at low temperatures. Especially for graphite, as a prototype of a weakly interacting substrate, this question is unsettled; even though a large amount of studies concerning metal clusters on graphite have been published so far [3–17], this problem was rarely addressed.

This was our motivation to investigate the temperature dependent growth mode of a metal on this substrate. Nickel was chosen since the lattice constant of the (111) plane (2.49 Å) is almost identical with the lattice constant of the basal plane of graphite (2.46 Å), and it is interesting to know whether this leads to some kind of epitaxial growth on condition that thermodynamic equilibrium cannot be reached.

For the structural characterisation of the metal aggregates, SPA-LEED (spot profile analysis LEED) was used. This method has the advantage that it does not induce structural changes as might be expected with other techniques (TEM, STM, AFM) when investigating clusters on weakly interacting substrates. Moreover, XPS (X-ray photoelectron spectroscopy)

* Corresponding author. Fax: +49 234 7094182.

SSDI 0039-6028(94)00855-8

data were taken in order to get additional information, e.g. concerning the metal coverages.

2. Experimental

We performed the experiments in two different ultrahigh vacuum systems. The LEED investigations were carried out with a Leybold SPA-LEED system (specified transfer width: 900 Å, typical primary beam currents: 50 pA–1 nA). The chamber also contained a conventional LEED optics and a quadrupole mass spectrometer for residual gas analysis. The XPS data were taken in a spectrometer equipped with a monochromatised Al Kα source (Leybold). Again, a LEED optics and a QMS were available.

The sample we used was highly oriented pyrolytic graphite (HOPG, Union Carbide, grade: ZYA). This synthetic material is not single crystalline but has properties which are in many cases identical to those of a single crystal [18]. This is due to its structure: HOPG consists of small crystallites (~ 1 μm) [19], which have been aligned with respect to their basal planes during the production process. However, a common orientation with respect to the crystallographic directions within the planes is missing. If such a sample is investigated with LEED, rings instead of spots are observed in the first and the higher diffraction orders [20].

In spite of this disadvantage, we preferred HOPG to a graphite single crystal since single crystals usually have a pronounced mosaic structure leading to broad or multiple LEED spots. In contrast to that, the mosaic spread of HOPG is small leading to sharp diffraction features. Via SPA-LEED we determined a mean tilting angle of 0.2° for the basal planes of the crystallites in accordance with the specification of the manufacturer.

The sample holder is depicted in Fig. 1. Via a Mo frame and Mo screws, the crystal was attached to two Ta rods. These rods were connected to a liquid nitrogen reservoir allowing cooling of the sample to 90 K. Heating was possible by radiation from the filaments or by electron bombardment onto the reverse side of the crystal.

As described in the literature [21], a clean graphite surface was obtained by cleaving the crystal with scotch tape. After transfer into the vacuum system it was additionally heated to 1000°C for 15 min. In the following any ion bombardment of the sample was carefully avoided: Metois et al. demonstrated [13] that even low energy ions as produced by ion getter pumps and ionisation gauges create point defects which eventually act as nucleation sites for the growth of metal clusters.

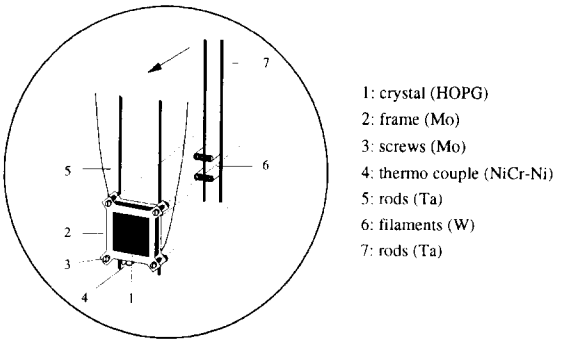

Fig. 1. Mounting of the HOPG crystal.

Nickel was evaporated with the help of a home-built Knudsen cell. The evaporator had an efficient water cooling system so that the pressure never exceeded 2×10^{-10} mbar during operation.

We have studied the growth behaviour of Ni at two substrate temperatures: 90 K (cooling with liquid nitrogen) and 300 K (ambient temperature). The evaporation rate we employed amounted to 1.9×10^{11} atoms per second and mm^2 (~ 0.01 ML/s). Since the sticking probability for metals on graphite is unknown [22], only the deposition times will be given at first. For deposition at 90 K the corresponding coverages as determined by XPS will follow in Section 3.2.

Removal of Ni from the surface was easily achieved by heating the sample to 1000°C for several minutes. After that treatment the Ni concentration on the surface was below 0.15%.

3. Results and discussion

3.1. SPA-LEED results

Before going into the details of the LEED profile analysis, it is important to mention that extra diffrac-

tion rings due to a Ni-induced superstructure have never been observed upon deposition of Ni on graphite. This can be considered as a first clue to a growth of Ni islands with a lattice constant identical to that of the substrate. Nevertheless, it should be kept in mind that this result may also be the consequence of disordered or irregularly shaped clusters.

Due to the low intensity of the higher-order diffraction features, an elaborate spot profile analysis was only possible for the mirror reflex. Nevertheless, as will become evident, the (00) beam spot profile contains enough information to clarify the growth behaviour, which will be discussed first for deposition at 90 K and then for deposition at room temperature.

During the experiments at low temperature, it was recognised that the surface structure is not stable directly after evaporation of Ni. The changes in the spot profiles, shown in Fig. 2 for an electron energy of 35 eV (deposition time: 550 s), demonstrate that some kind of structural rearrangement takes place on the surface. Obviously, the sharp spike visible in the centre of the profiles gains intensity. Besides, the other component, a diffuse shoulder, changes from a ring-shaped into a Lorentzian profile. It always took approximately two hours to reach the final form of the profiles. However, this development was only observed at two energies: in the energy range between 35 and 80 eV – higher electron energies could not be investigated since the spot intensity was too low (cf. $I(V)$ curve (integrated spot intensity versus energy) in Ref. [23]), and lower energies were unsuitable because of experimental artifacts – these effects were merely observed at 35 and 80 eV. At other energies only slight changes occurred.

In order to explain this result, it is useful to discuss the final shape of the profiles first. As can be seen in Fig. 3, where an energy series is depicted, the profiles show a strong energy dependence. However, all of them could be separated into a sharp Gaussian part, resembling the profile of the clean substrate, and a broad shoulder, which is a unique feature of the metal covered surface. A representative least-squares fit is presented in the inset of the figure.

It is known from literature that inhomogeneous

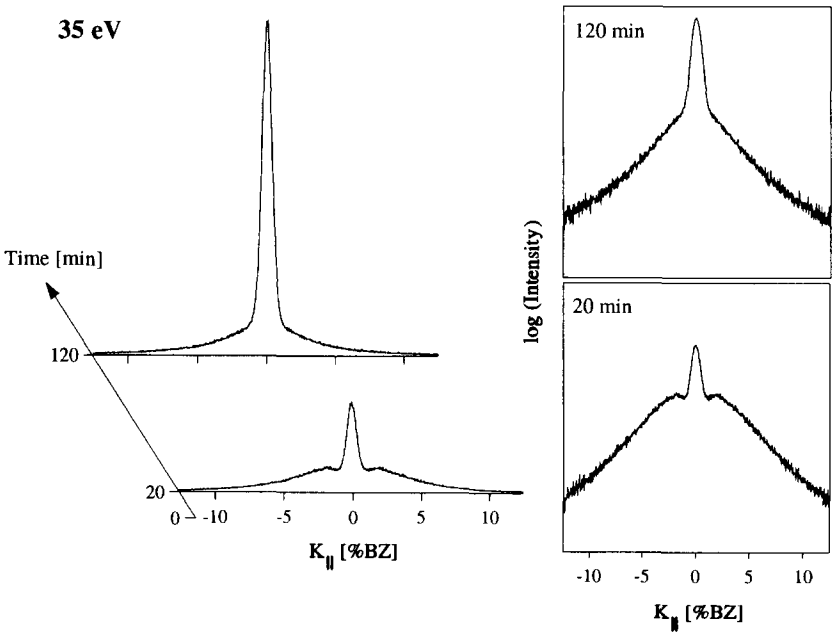

Fig. 2. Profiles of the (00) LEED spot for an electron energy of 35 eV as a function of time after depositing Ni for 550 s at 90 K. A similar development of the spot profiles at that energy was observed for shorter deposition times as well. The parallel component of the scattering vector on the X-axis is given in percent of the Brillouin zone of graphite.

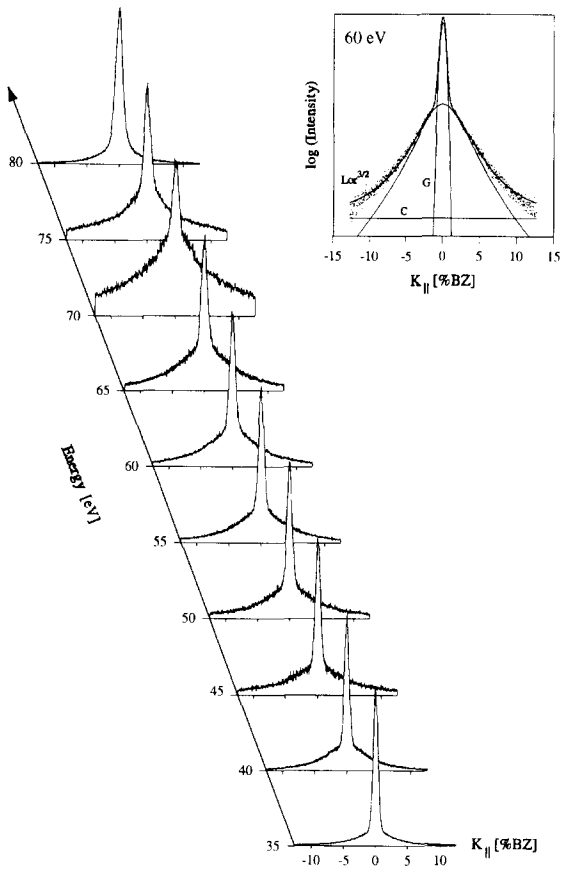

Fig. 3. Spot profiles as a function of energy for the deposition at low temperature (550 s). The profiles have been recorded approximately two hours after the evaporation. The inset shows a representative least-squares fit of the profile at 60 eV (G: Gaussian function, $Lor^{3/2}$: modified Lorentzian function, C: constant background).

surfaces like ultrathin heteroepitaxial films result in spot profiles as those observed here [24]. Briefly, the central peak is due to in-phase scattering between different layers, while the shoulder is the consequence of out-of-phase scattering. Since the condition for in- and out-of-phase scattering varies with energy, the intensity ratio between the peak and the shoulder is also a function of energy. A schematic picture of a three-dimensional heteroepitaxial island is depicted is Fig. 5a. If the terrace lengths L, as defined there, correspond to two-dimensional isotropic, geometric distributions, the shoulder consists of several Lorentzian-type functions ($f_{(K_{parallel})}$ = (Lorentzian)$^{3/2}$), the number of which is given by the number of layers minus one [25,26].

In Fig. 4a the part of the total integrated intensity found in the Gaussian peak is plotted versus the energy. It is obvious that the highest intensities and therefore maxima for in-phase scattering are reached at 35 and 80 eV, where previously the most pronounced temporal changes were observed.

Furthermore, the full widths at half maximum (FWHM) of peak and shoulder have been determined. Whereas the halfwidth of the Gaussian function is equivalent to that measured for the clean graphite surface, the halfwidth of the shoulder, as shown in Fig. 4b, appears to have minima at 35 and 80 eV.

The structure of the metal deposit follows immediately from these findings when considering that 35 and 80 eV are quite close to two in-phase energies of Ni(111) (36.8, 82.9 eV). Bearing this in mind, the only possible explanation for both the temporal changes described above and the results shown in

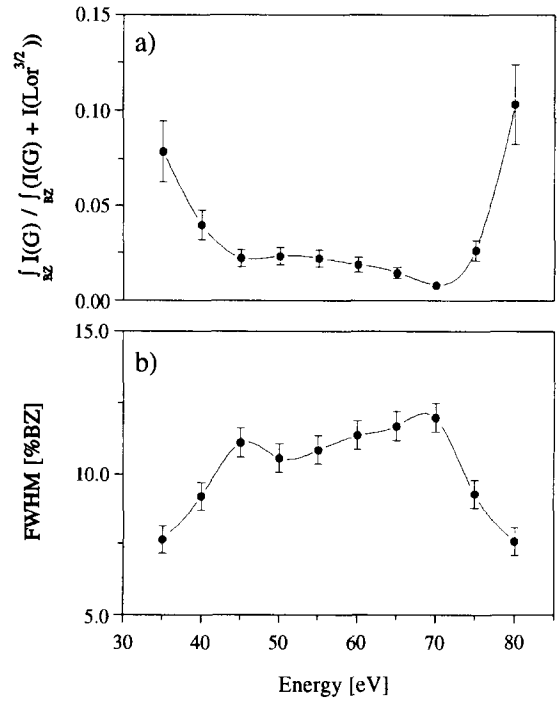

Fig. 4. Integrated intensity of central peak in relation to the total spot intensity (a) and full width at half maximum of the $Lor^{3/2}$ shoulder (b) at different energies (deposition time: 550 s).

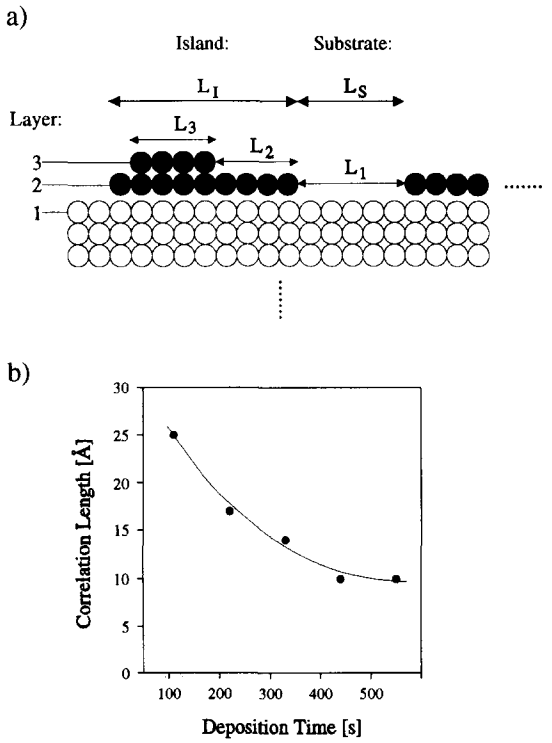

Fig. 5. (a) Definition of terrace lengths for three-dimensional heteroepitaxial islands. (b) Plot of the correlation lengths L as calculated from the FWHM of the $Lor^{3/2}$ shoulder at 35 and 80 eV (see Table 1). L results from $\bar{L}_I$ and $\bar{L}_S$ as given by Eq. (1).

Fig. 4 is the formation of three-dimensional Ni(111) islands: since all Ni layers in such islands scatter in phase at the specific Ni(111) in-phase energies, maxima of the intensity of the central peak are expected here. In addition to that, minima of the halfwidth of the shoulder should be found at these points due to the absence of the Lorentzians connected with the metal layers above the first layer. If the Ni(111) islands are emerging slowly, the accompanying temporal changes ought to be most pronounced at the corresponding in-phase energies as it was indeed observed in the present case. Therefore, all results corroborate the idea of epitaxial Ni(111) islands growing slowly on the surface.

Concerning Fig. 4a, one aspect so far not addressed ought to be mentioned finally: it might be surprising that even at 35 and 80 eV the intensity of the central peak is merely around 10% of the total intensity. However, the occurrence of destructive interference of electrons scattered at the islands on the one hand and at the substrate on the other hand has to be taken into consideration. Apparently, this part always plays the dominant role for the LEED spot profiles. Note that this contribution cannot be analysed with elementary kinematic scattering theory [24]. This is because of the different atomic scattering factors for Ni and graphite and their unknown energy dependence. Therefore, a more elaborate profile analysis, as it is possible for homoepitaxial systems [27,28], cannot be carried out here.

We have furthermore investigated the behaviour for lower coverages (deposition times between 110 and 440 s), and similar effects have been observed in all cases. Hence, it can be concluded that the growth behaviour described is typical of deposition at low temperature.

On the basis of the qualitative picture established so far, the data can also be used to get some quantitative information concerning the arrangement of the metal aggregates on the surface. Although it is impossible to extract the exact size of the islands, the data allow the determination of the correlation length L of the two-dimensional pattern originating from the distribution of metal covered and uncovered areas on the surface. This quantity depends on both the mean lateral extensions of the free graphite patches $\bar{L}_S$ and of the islands $\bar{L}_I$ (see Fig. 5a). Approximately, the following equation is valid [28]:

$$1/L = 1/\bar{L}_s + 1/\bar{L}_I. \quad (1)$$

The correlation length L can be calculated from the halfwidths of the Lorentzian$^{3/2}$ shoulder at the Ni(111) in-phase energies:

$$L = \sqrt{2^{2/3} - 1}\ 2/\mathrm{FWHM}. \quad (2)$$

At these energies the profiles of the Ni(111) islands are of course identical to profiles of two-dimensional Ni islands with a lateral extension $\bar{L}_I$ due to in-phase scattering between all Ni layers.

The results are summarised in Table 1 and graphically displayed in Fig. 5b. Obviously, the correlation length of the arrangement decreases with increasing deposition time. Taking Eq. (1) into account, this must be a consequence of the mean distance between the islands $\bar{L}_S$ becoming smaller since it is unreasonable to assume instead that the mean lateral exten-

sion of the islands $\bar{L}_I$ declines when increasing the metal coverage. On the other hand, L should decrease of course at coverages smaller than those studied here due to small island diameters $\bar{L}_I$. However, shorter deposition times have not been employed for this investigation: in this case the shoulder had too little intensity to allow for a reliable fitting procedure.

When depositing Ni at 300 K, the spot profiles have a totally different shape. An energy series analogous to Fig. 3 is shown in Fig. 6 for a deposition time of 550 s. In contrast to the preparation at low temperature, a decomposition into a central part and a shoulder is impossible. However, the inset in Fig. 6 reveals that a drastic increase of the halfwidths is detected.

Since the overall appearance of the profiles does not change with energy and nearly all half-widths are affected in a similar way, it may be assumed that the inner structure of the metal aggregates does not play a role for the spot profiles of the (00) beam. With respect to their influence on the mirror reflex, they could therefore be considered as "black holes" on the surface [24]. This would point to metal clusters having irregular shapes or several facets. This interpretation is also supported by the $I(V)$ curves (integrated spot intensity versus energy) of the metal covered samples, as their shapes are identical with that of the clean substrate.

Anyway, since a diffuse shoulder, as always expected for an inhomogenous surface [24], cannot be separated from the central spike, its FWHM must be comparable to the FWHM of the central peak. According to Eqs. (1) and (2), this means that the lateral extension of the clusters as well as the distances between them must be much larger than at 90 K.

Table 1
Correlation length as calculated from the FWHM of the $Lor^{3/2}$ shoulder at 35 and 80 eV

Deposition time (s)	FWHM (%BZ)	Correlation length (Å)
110	3.1	25
220	4.6	17
330	5.6	14
440	8.2	10
550	7.6	10

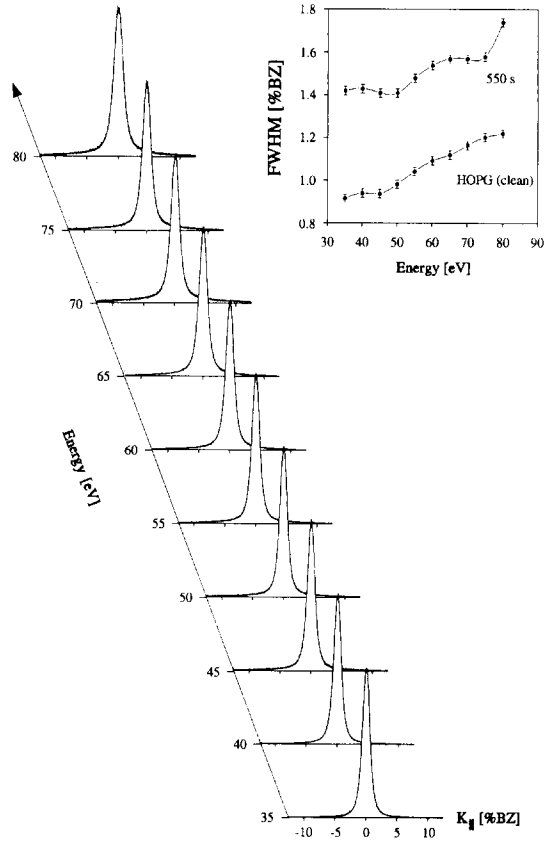

Fig. 6. Energy series of the LEED spot profiles obtained after deposition of Ni at room temperature (550 s). Inset: full width at half maximum of the profiles as a function of energy before and after deposition. The monotonous increase of the halfwidths in both cases is owing to the mosaic structure of the substrate. The additional oscillations have been identified as instrumental artifacts in the case of the clean substrate.

In this context it is worth mentioning that the islands at 90 K do not convert into the larger clusters when warming up the sample to 300 K: in this case only slight changes were observed in the spot profiles as compared to the original profiles recorded at 90 K. Particularly, the overall shape consisting of a sharp and a diffuse part was still clearly visible.

3.2. XPS data

Fig. 7 shows a typical Ni 2p spectrum obtained after deposition of Ni at 90 K. It is also representative of the spectra recorded after deposition at 300 K. When comparing it to the corresponding spectrum of

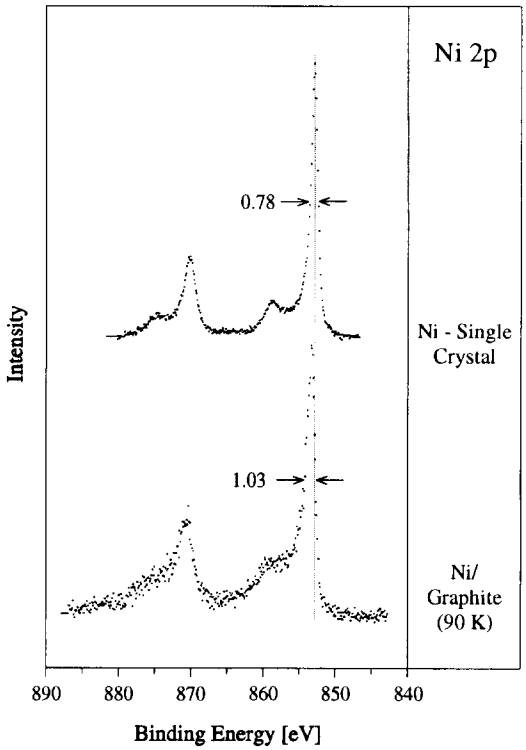

Fig. 7. Comparison between the Ni 2p spectra of a Ni(111) single crystal and Ni deposited on graphite (330 s, 90 K). The first spectrum was recorded with a transmission energy of 25 eV, the second with a transmission energy of 50 eV (loss of resolution by a factor of 1.2).

a Ni single crystal, also presented in Fig. 7, two important differences are noticeable. First, the spectrum of the clusters is slightly shifted towards higher binding energy (larger shifts for deposition at 90 K) and, second, it is broader than the spectrum of the single crystal (even when the higher transmission energy is taken into account!).

Both phenomena are well known for small clusters on weakly interacting substrates [29,30]. Whereas the large halfwidths are generally believed to be due to a broad distribution of binding energies resulting from a corresponding distribution of cluster sizes, the binding energy shifts themselves are caused either by final or by initial state effects during the photoemission process as discussed in the literature [29,30]. However, this aspect was not of central interest for this investigation and will not be dealt with further here.

We have instead focused on the Ni 2p and C 1s intensities in order to get information concerning the metal coverages on the surface. Assuming that the metal aggregates have the shape of flat islands with the height h covering a fraction θ of the surface, the XPS intensities are given by:

$$I(\mathrm{C\ 1s}) = I_0 - \theta I_0\{1 - \exp[-h/(\lambda(\mathrm{C\ 1s})\cos\alpha)]\}, \quad (3)$$

$$I(\mathrm{Ni\ 2p}) = \theta I_\infty\{1 - \exp[-h/(\lambda(\mathrm{Ni\ 2p})\cos\alpha)]\}, \quad (4)$$

where I_0 is the C 1s intensity of the clean sample, I_∞ is the Ni 2p intensity of a thick Ni film, and λ is the mean free path of the electrons with the respective kinetic energies. According to Seah et al. [31], an estimated value for λ may be calculated from the following equation:

$$\lambda/\mathring{A} = 1430(E/\mathrm{eV})^{-2} + 0.54\sqrt{E/\mathrm{eV}}. \quad (5)$$

Taking into account that the islands grown at low temperature are composed of Ni layers aligned parallel to the substrate, this model may be used for a quantitative evaluation, even if the islands are not flat but consist of several terraces: in this case the quantity h represents a kind of mean island height. However, it is certainly not appropriate for the clusters grown at 300 K. Therefore, the corresponding XPS data have not been analysed. The results which have been obtained for the Ni(111) islands by using Eqs. (3)–(5) and neglecting diffraction phenomena are summarised in Table 2.

Table 2
Quantitative evaluation of the XP data: h is the island height and θ is the fraction of the surface covered with Ni (see text)

Deposition time (s)	Island height h (Å)	Coverage θ
110	5.3	0.19
220	6.0	0.37
330	6.1	0.50
440	6.0	0.59
550	6.0	0.70

For the calculation data taken at two collection angles (0° and 74.4°) were used. All values should only be considered as guidelines.

The most remarkable aspect of this survey is the island height being identical for deposition times longer than 110 s. The value of about 6 Å hints at three Ni layers building up the islands (interlayer distance: 2.03 Å), but this number as well as the coverages should only be taken as guidelines because of the approximations included in the model.

4. Summary and conclusions

We have studied the growth behaviour of nickel on the basal plane of graphite at 90 K and at 300 K (ambient temperature):

(i) At 90 K the formation of three-dimensional Ni(111) islands has been observed. Their growth, however, is a slow process taking place within two hours after deposition. It is likely that the islands have a constant height independent of the metal coverage.

(ii) In contrast to that, the deposition of Ni at 300 K results in clusters being much larger than the Ni(111) islands at 90 K. No indication for a preferred crystallographic orientation has been found in this case.

Certainly, the driving force for the formation of the epitaxial islands at 90 K is the small mismatch between the lattice constant of Ni(111) and the lattice constant of graphite. This is also supported by a study of Fan et al. [32], who have investigated the growth of Al on graphite in the temperature range between 80 and 400 K. They could not find any evidence for Al islands with a preferential crystallographic orientation.

Since the preparation of the (111) islands is only possible at low temperatures, it is reasonable to assume that their formation is a kinetically controlled process. Under these circumstances the weak interaction between substrate and metal is able to determine the growth behaviour. On the other hand, a Vollmer–Weber growth mode, where the forces between the metal atoms are dominating, is expected for graphite as a weakly interacting substrate if it is possible to reach the thermodynamic equilibrium. The clusters observed at 300 K seem to belong to that growth mode and therefore probably represent the thermodynamically stable situation.

Acknowledgements

Financial support of the following agencies is gratefully acknowledged: Deutsche Forschungsgemeinschaft, Ministerium für Wissenschaft und Forschung des Landes Nordrhein-Westfalen, Bundesministerium für Forschung und Technologie, Fonds der chemischen Industrie. Furthermore, M.B. thanks the Studienstiftung des deutschen Volkes for a fellowship. M.B. is also grateful to Professor M. Henzler and Dr. J. Wollschläger (Hannover) for helpful discussions.

References

[1] M. Zinke-Allmang, L.C. Feldman and M.H. Grabow, Clustering on Surfaces, Surf. Sci. Rep. 16 (1992) 377.
[2] R. Kern, G. Le Lay and J.J. Metois, Basic Mechanisms in the Early Stages of Epitaxy, in: Current Topics in Material Science, Vol. 3, Ed. E. Kaldis (North-Holland, Amsterdam, 1979).
[3] E. Ganz, K. Sattler and J. Clarke, Surf. Sci. 219 (1989) 33.
[4] E. Ganz, K. Sattler and J. Clarke, Phys. Rev. Lett. 60 (1988) 1856.
[5] E. Ganz, K. Sattler and J. Clarke, J. Vac. Sci. Technol. A 6 (1988) 419.
[6] D.W. Abraham, K. Sattler, E. Ganz, H.J. Mamin, R.E. Thomson and J. Clarke, Appl. Phys. Lett. 49 (1986) 853.
[7] M. Kuwabara, D.A. Smith and D.R. Clarke, J. Appl. Phys. 68 (1990) 6520.
[8] U. Müller, K. Sattler, J. Xhie, N. Venkateswaran and G. Raina, J. Vac. Sci. Technol. B 9 (1991) 829.
[9] A. Humbert, M. Dayez, S. Sangay, C. Chapon and C.R. Henry, J. Vac. Sci. Technol. A 8 (1990) 311.
[10] A. Humbert, M. Dayez, S. Granjeaud, P. Ricci, C. Chapon and C.R. Henry, J. Vac. Sci. Technol. B 9 (1991) 804.
[11] V. Maurice and P. Marcus, Surf. Sci. 275 (1992) 65.
[12] T. Ngo, L. Brandt, R.S. Williams and H.D. Kaesz, Surf. Sci. 291 (1993) 411.
[13] J.J. Metois, J.C. Heyraud and Y. Takeda, Thin Solid Films 51 (1978) 105.
[14] J.F. Hamilton and P.C. Logel, Thin Solid Films 16 (1973) 49.
[15] J.F. Hamilton and P.C. Logel, Thin Solid Films 23 (1974) 89.
[16] K. Heinemann and H. Poppa, Thin Solid Films 33 (1976) 251.
[17] M.A. Listvan, Surf. Sci. 173 (1986) 294.
[18] A.W. Moore, Highly Oriented Pyrolytic Graphite, in: Chemistry and Physics of Carbon, Vol. 11, Eds. P.L. Walker and P.A. Thrower (Dekker, New York, 1973) p. 69.
[19] S. Morita, S. Tsukada and N. Mikoshiba, J. Vac. Sci. Technol. A 6 (1988) 354.

[20] A.G. Roosenbrand, M.W.C. van Beckhoven and H.H. Brongersma, Appl. Surf. Sci. 44 (1990) 121.
[21] R.G. Musket, W. McLean, C.A. Colmenares, D.M. Makowiecki and W.J. Siekhaus, Appl. Surf. Sci. 10 (1982) 150.
[22] J.R. Arthur and A.Y. Cho, Surf. Sci. 36 (1973) 641.
[23] J.J. Lander and J. Morrison, J. Appl. Phys. 35 (1964) 3593.
[24] J. Wollschläger, J. Falta and M. Henzler, Appl. Phys. A 50 (1990) 57.
[25] C.S. Lent and P.I. Cohen, Surf. Sci. 139 (1984) 121.
[26] J. Wollschläger, E.Z. Luo and M. Henzler, Phys. Rev. B 44 (1991) 13031.
[27] M. Horn, U. Gotter and M. Henzler, J. Vac. Sci. Technol. B 6 (1988) 727.
[28] J. Wollschläger and M. Henzler, Phys. Rev. B 39 (1989) 6052.
[29] M.G. Mason, Phys. Rev. B 27 (1983) 748.
[30] G.K. Wertheim, Z. Phys. B 66 (1987) 53.
[31] M.P. Seah and W.A. Dench, Surf. Interface Anal. 1 (1979) 2.
[32] W.C. Fan, J. Strozier and A. Ignatiev, Surf. Sci. 195 (1988) 226.